Baggio, M.; Tamminen, A.; Ala-Laurinaho, J.; Wallace, V. P.; Taylor, Z. D.

Design of a ring-focus dual reflector objective for standoff sensing of spherical targets in the 220 - 330 GHz band

Published in:
IRMMW-THz 2022 - 47th International Conference on Infrared, Millimeter and Terahertz Waves

DOI:
10.1109/IRMMW-THz50927.2022.9895473

Published: 01/01/2022

Document Version
Peer-reviewed accepted author manuscript, also known as Final accepted manuscript or Post-print

Design of a ring-focus dual reflector objective for standoff sensing of spherical targets in the 220 – 330 GHz band

M. Baggio[1], A. Tamminen[1], J. Ala-Laurinaho[1], V.P. Wallace[2] and Z. D. Taylor[1]
[1]Department of Electronics and Nanoengineering, MilliLab, Aalto University, 02150 Espoo, Finland
[2]Department of Engineering and Mathematical Sciences, University of Western Australia, Crawley, WA, 6009, Australia

***Abstract*—A dual reflector objective design is explored in WR-3.4 for sensing of spherical targets. The secondary mirror shadow enables coaxial integration of topical systems without additional obscuration of the submillimeter wave beam. The system is designed with geometrical optics and evaluated with physical optics. The power coupling efficiency between the source electric field and back scattered field from a spherical target is > 0.4 across the frequency of interest.**

I. Introduction

Submillimeter sensing is under active research as a candidate *in vivo* corneal water sensing. Ozheredov et al. reported *in vivo* sensing of the tear film physiological dynamics and corneal hydration [1]. Chen et al. investigated the water dynamics in corneal phantoms [2], and Yao et al. studied corneal water extraction from *ex vivo* samples [3]. Further, the dielectric properties of cornea both *in vivo* and *ex vivo* samples were reported on by Mizuno et al. [4].

We have designed several optical systems for cornea sensing including an off-axis parabolic mirror quasioptical bench [5], a Gaussian beam telescope [6], and an axicon lens [7]. This work utilized optical (visible and near infrared) assessment of phantom geometry and, in the case of [6], and [7] integrated optical coherence tomography (OCT) into the work flow.

We recently started to investigate dual reflector objectives that allow the integration of an adjunct OCT system in the obscuration introduced by its secondary mirror [8]. In this abstract, we explore a dual reflector design where the two mirror surfaces are generated by the rotation of ellipse arcs around the optical axis. In the literature, similar designs have been presented for dual reflector antennas [9-11] or telescopes which, more generally, often rely on conic sections. The design goal is wavefront matching on a cornea-like target, to simplify the inverse scattering problem and extract the cornea constituent parameters.

II. Design and Results

As a first step, we assumed that both the source and objective focus are infinitesimal points. Geometrical arguments were then used to guide the design. The arrangement can be visualized on a 2D plane, as the overall optical system is rotationally symmetric. Ellipses are curves, synthesized so that the sum of the distances between a point of the curve and two fixed internal points (the foci) is constant and it is twice the semi-major axis. Furthermore, rays traced from one of the foci to any region of the elliptical surface are reflected back to the other focus. These two facts ensure that the optical path length (OPL) from one focus to the other is constant for all rays independent to their departure direction from the source focus. Moreover, if the target has a spherical surface, whose center of curvature is co-located with the imaging focus, the OPL from source point to spherical surface is constant. A constant OPL for all rays indicates perfect wavefront matching from a geometric optics point of view and suggests low wavefront error for longer, i.e. submillimeter wavelengths. These features support the design as a good starting point for pursuing the desired wavefront matching condition. The final step is to combine the arcs of two tilted ellipses with one common focus and rotate them around the optical axis as in Fig. 1. The ellipse arcs are therefore acting as generatrix curves for the objective mirrors.

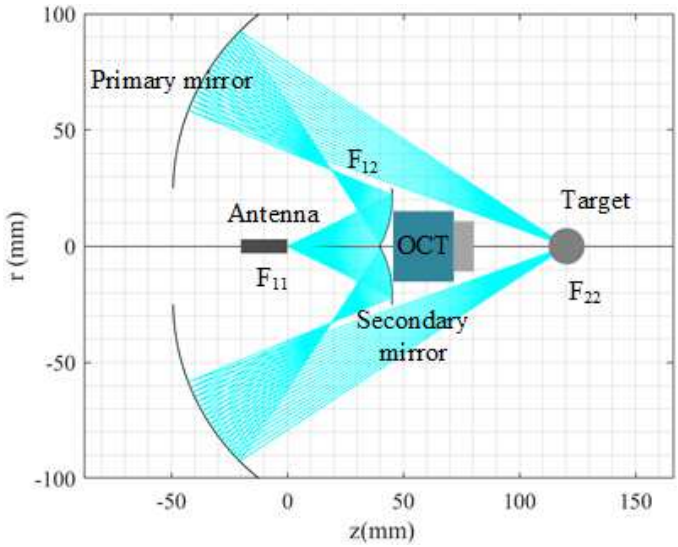

Fig. 1. Setup cut on a sagittal plane. The first ellipse generatrix (for secondary mirror) has one focus at the antenna waist location (F_{11}). The second ellipse generatrix (for primary mirror) is located so that it has one focus in common with the other generatrix (F_{12}) and the other focus on the optical axis (F_{22}). The sphere center of curvature is co-located with the latter focus. Rays have been traced sequentially from the antenna waist location to the sphere surface.

This first approximation for the geometric wavefront matching enables a somewhat independent exploration of the design dimensions. Thus, the secondary mirror was sized to theoretically fit an adjunct OCT objective in its shadow. Further, the secondary mirror distance to the antenna and primary mirror diameter were set to limit spillover on both mirrors. Additionally, the ellipses need to have a common focus (F_{12}), which will become the ring focus, and the rays from the primary to the final focus should clear the secondary mirror with minimal clipping. The secondary mirror has diameter 50 mm to ensure that the obscuration can fit an OCT device, and its generatrix is an ellipse with semi-major axis of 39.3 mm, linear eccentricity of 19 mm, and rotation angle of 60°. The second ellipse has a diameter of 200 mm, and rotation angle of −18°, a semi-major axis of 120 mm, and a linear eccentricity of 53.2 mm.

The design was evaluated with an in-house Physical Optics

(PO) code in the WR-3.4 (220-330 GHz) band (Fig. 2).

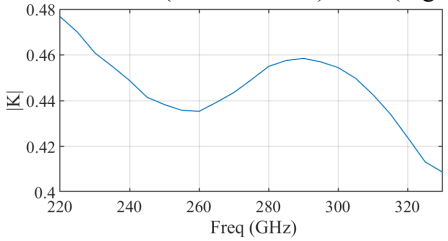

Fig. 2. (a) Amplitude of the power coupling coefficient in WR3.4.

The code sequentially integrates the vectorial form of the Kirchhoff's diffraction integral of the electric field from surface to surface. The system was fed with a Gaussian beam polarized along the x-axis. Fig. 2 shows the amplitude (a) and phase (b) of the electric field on a target at 275 GHz. The target is a spherical cap with a diameter of 12.5 mm and a radius of curvature of 7.8 mm and was modelled as a perfect electrical conductor (PEC). The amplitude shows the ring pattern as predicted by ray tracing, but with a maximum at the center, which is most likely the Arago or Poisson spot [12]. The phase variation is relatively limited in the area equivalent to the illuminated area in ray tracing. This is also addressed in Fig. 2c, which reports the phase along a frontal plane at all simulated frequencies. Here, the phase is represented as the phase difference between the obtained phase in PO and the phase corresponding to the OPL from the feed to the surface. The OPL to the cap surface is two times the sum of the semi-major axes minus the radius of curvature of the target. The translucent areas denote the area illuminated in ray tracing like in Fig. 1. In the translucent red area, the phase variation increases with increasing frequency. The power coupling efficiency between the electric field at the source and the field that is reflected back at the source is 0.48 at 220 GHz, 0.45 at 275 GHz, and 0.41 at 330 GHz (Fig. 2). Interestingly, this decreasing trend corresponds with the more degraded phase in Fig. 2c, where the 330-GHz curve has higher variation in the red area. The cause of this could be also the source definition as the beam waist, and therefore the gain, is frequency dependent as it was extracted from the beam pattern measurements of WR-3.4 horn antenna utilized in previous work [6].

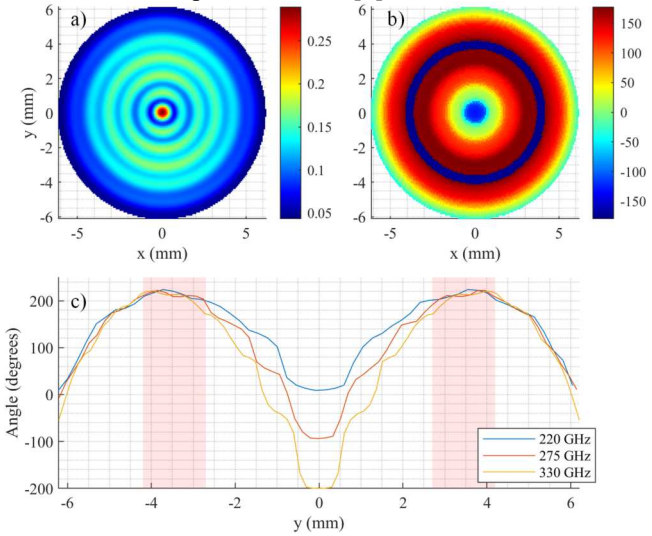

Fig. 3. (a) Amplitude and (b) phase of the co-polar component of the electric field on the spherical surface at 275 GHz. (c) Unwrapped phase difference between PO and ray tracing (OPL) along a frontal plane on the sphere at the three different frequencies.

CONCLUSION

A ring focus dual reflector has been studied. The design was dimensioned with geometrical optics and evaluated in PO showing preliminary promising results.

ACKNOWLEDGMENTS

This work is funded by Academy of Finland RADDESS program (project AGRUM, decision number 327640). We acknowledge the computer resources provided by the Aalto Science IT-Project.

REFERENCES

[1] I. Ozheredov *et al.*, "In vivoTHz sensing of the cornea of the eye," *Laser Physics Letters,* vol. 15, no. 5, p. 055601, 2018.

[2] A. Chen, O. B. Osman, Z. B. Harris, A. Abazri, R. Honkanen, and M. H. Arbab, "Investigation of water diffusion dynamics in corneal phantoms using terahertz time-domain spectroscopy," (in eng), *Biomed Opt Express,* vol. 11, no. 3, pp. 1284-1297, 2020.

[3] J. Yao *et al.*, "Corneal hydration assessment indicator based on terahertz time domain spectroscopy," *Biomed Opt Express,* vol. 11, no. 4, pp. 2073-2084, 2020.

[4] M. Mizuno *et al.*, "Dielectric property measurements of corneal tissues for computational dosimetry of the eye in terahertz band in vivo and in vitro," *Biomed Opt Express,* vol. 12, no. 3, pp. 1295-1307, 2021.

[5] Y. Hu *et al.*, "650 GHz Imaging as Alignment Verification for Millimeter Wave Corneal Reflectometry," *IEEE Transactions on Terahertz Science and Technology,* vol. 12, no. 2, pp. 151-164, 2022.

[6] A. Tamminen, S. V. Pälli, J. Ala-Laurinaho, M. Salkola, A. V. Räisänen, and Z. D. Taylor, "Quasioptical System for Corneal Sensing at 220–330 GHz: Design, Evaluation, and *Ex Vivo* Cornea Parameter Extraction," *IEEE Transactions on Terahertz Science and Technology,* vol. 11, no. 2, pp. 135-149, 2021.

[7] A. Tamminen, S. V. Pälli, J. Ala-Laurinaho, M. Salkola, A. V. Räisänen, and Z. Taylor, "Axicon-hyperbolic lens for reflectivity measurements of curved surfaces," in *2020 14th European Conference on Antennas and Propagation (EuCAP)*, 2020, pp. 1-5.

[8] M. Baggio, A. Tamminen, J. Ala-Laurinaho, and Z. Taylor, "Design of dual-reflector objective for corneal sensing in the 220 – 330 GHz band," presented at the 2022 16th Conference on Antennas and Propagation (EuCAP), Madrid, 2022.

[9] C. Granet, "A simple procedure for the design of classical displaced-axis dual-reflector antennas using a set of geometric parameters," *IEEE Antennas and Propagation Magazine,* vol. 41, no. 6, pp. 64-72, 1999.

[10] G. Wu, S. Qu, S. Yang, and C. Ma, "Design of Cassegrain reflectarray antenna with compact ring focus feed," in *2017 11th European Conference on Antennas and Propagation (EUCAP)*, 2017, pp. 978-980.

[11] A. Kezuka, K. Igarashi, and G. Yoshida, "Dielectric guide cassegrain antennas with ring focus parabolic reflector," in *2010 Asia-Pacific Microwave Conference*, 2010, pp. 1981-1984.

[12] J. W. Goodman, *Introduction to Fourier Optics*, 3rd ed.: W. H. Freeman, 2005, p. 34.